

RESEARCH

Open Access



LncRNA NORFA promotes the synthesis of estradiol and inhibits the apoptosis of sow ovarian granulosa cells through SF-1/CYP11A1 axis

Zhennan Guo^{1†}, Qiang Zeng^{1†}, Qiqi Li^{1,2}, Baosen Shan¹, Yangan Huo¹, Xiaoli Shi^{1,3}, Qifa Li¹ and Xing Du^{1*}

Abstract

Background Biosynthesis of 17 β -estradiol (E2) is a crucial ovarian function in mammals, which is essential for follicular development and pregnancy outcome. Exploring the epigenetic regulation of E2 synthesis is beneficial for maintaining ovary health and the optimal reproductive traits. NORFA is the first validated sow fertility-associated long non-coding RNA (lncRNA). However, its role on steroidogenesis is elusive. The aim of this study is to investigate the regulation and underlying mechanism of NORFA to E2 synthesis in sow granulosa cells (GCs).

Results Through Pearson correlation analysis and comparative detection, we found that NORFA expression was positively correlated with the levels of pregnenolone (PREG) and E2 in follicles, which also exhibited similar alteration patterns during follicular atresia. ELISA was conducted and indicated for the first time that NORFA induced the synthesis of PREG and E2 in sow GCs in a dose- and time-dependent manner. RNA-seq, GSEA and quantitative analyses results validated that *CYP11A1*, the coding gene of P450SCC which is the first step rate-limiting enzyme of E2 synthesis, was a positive functional target of NORFA. Mechanistically, NORFA promotes SF-1 expression by stabilizing NR5A1 mRNA through directly interacting with its 3'-UTR, and also tethers SF-1 to shuttle into nucleus. Additionally, SF-1 in the nucleus activates *CYP11A1* transcription by directly binding to its promoter, which ultimately induces E2 synthesis and inhibits GC apoptosis.

Conclusion Our findings highlight that NORFA, a multifunctional lncRNA, induces E2 synthesis and inhibits GC apoptosis through the SF-1/CYP11A1 axis in a ceRNA-independent manner, which provide valuable clues and potential targets for follicular atresia inhibition and female fertility improvement.

Keywords E2 synthesis, Sow granulosa cells, NORFA, *CYP11A1*, SF-1, Apoptosis

[†]Zhennan Guo and Qiang Zeng contributed equally to this work.

*Correspondence:

Xing Du
duxing@njau.edu.cn

¹College of Animal Science and Technology, Nanjing Agricultural University, Nanjing, Jiangsu 210095, China

²College of Animal Husbandry and Veterinary Medicine, Jiangsu Vocational College of Agriculture and Forestry, Zhenjiang, Jiangsu 212400, China

³National Experimental Teaching Demonstration Center for Animal Science, Nanjing Agricultural University, Nanjing, Jiangsu 210095, China



© The Author(s) 2024. **Open Access** This article is licensed under a Creative Commons Attribution-NonCommercial-NoDerivatives 4.0 International License, which permits any non-commercial use, sharing, distribution and reproduction in any medium or format, as long as you give appropriate credit to the original author(s) and the source, provide a link to the Creative Commons licence, and indicate if you modified the licensed material. You do not have permission under this licence to share adapted material derived from this article or parts of it. The images or other third party material in this article are included in the article's Creative Commons licence, unless indicated otherwise in a credit line to the material. If material is not included in the article's Creative Commons licence and your intended use is not permitted by statutory regulation or exceeds the permitted use, you will need to obtain permission directly from the copyright holder. To view a copy of this licence, visit <http://creativecommons.org/licenses/by-nc-nd/4.0/>.

Introduction

It is well-known that the fertility of female mammals depends on the follicular development, maturation, and ovulation [1], which are regulated by a complicated and precise network consisting of multiple in vivo and in vitro factors, including environment, nutrition, stress, cytokines, and steroid hormones [2–5]. Estrogens, an important kind of steroid hormones, are widely synthesized in female reproductive system and involved in the regulation of multiple physiological and pathological processes [6, 7]. As the most common form of estrogen with the highest activity, E2 is converted from cholesterol (CHOL) in ovarian GCs under the action of a series of rate-limiting enzymes [8], which is essential for the development of female reproductive system and determination of the follicular fate.

Clinical studies and mouse models showed that abnormal synthesis of E2 was closely associated with multiple reproductive disorder diseases, and lead to delayed ovarian development, sexual characteristics degeneration, follicular cysts, atresia, and anovulation, which impaired female fertility [9–11]. In addition to women and female mice, E2 levels in healthy follicles were also found to be significantly higher than those in atretic follicles and corpus luteum in domestic animals such as sows, cows, and sheep [12–14]. Therefore, E2 synthesis is one of the most crucial functions of GCs in female mammals, and low level of E2 in follicular fluid has been considered as a main feature of atretic follicles. However, the studies on E2 in sows and other large domestic animals are limited, especially its synthetic regulation is not fully understood. Potential endogenous candidates that can be utilized to maintain E2 synthesis, induce follicular development, and improve sow fertility need to be investigated.

With the improvement of intensive breeding, increasing studies have investigated the regulation of E2 synthesis in sows and identified a series of regulators, including in vitro and in vivo factors. The former contains endocrine disrupting chemicals (DDT etc.) [15], toxins (ZEN etc.) [16], antibiotics (VA etc.) [17], and viruses (PRV etc.) [18]. While, the latter mainly consists of hormones (FSH etc.) [19], cytokines (ULCH1 etc.) [20], homeostasis (ROS etc.) [21], and epigenetic regulators. miRNAs, an important kind of epigenetic regulator, have been reported to regulate E2 synthesis in sow ovaries, and 17 validated functional miRNAs have been identified in the last decade. For instance, miR-1275 inhibits E2 synthesis in the GCs from Yorkshire sows by directly targeting and suppressing *LHR-1* [22]. Conversely, miR-339 enhances E2 synthesis in sow GCs by acting as a small activating RNA (saRNA) which induces the transcription of *CYP19A1*, the coding gene of key rate-limiting enzyme P450arom [23]. Unlikely, it remains largely unknown about the regulation of lncRNAs on E2 synthesis in sow

ovaries. lncRNAs, another important class of widely-expressed endogenous non-coding RNAs with length longer than 200 nt and lack protein-coding potential [24], have been reported involved in various physiological and pathological processes in humans and rodents, including reproductive disorders such as polycystic ovary syndrome (PCOS) and ovarian cancer [25, 26]. However, only three validated lncRNAs (NORSE, IFFD, and SFFD) with the ability to influence E2 synthesis in sows have been identified at present [23, 27, 28]. Mechanism analyses have shown that they regulate E2 synthesis by directly sponging the downstream miRNAs, which is well-known as competitive endogenous RNA (ceRNA) mechanism. Despite them, additional functional lncRNAs that regulate E2 synthesis independent of ceRNA mechanism need to be identified.

Our previous study has identified NORFA as the first anti-atretic lncRNA associated with sow fertility [29]. Further RNA-seq and bioinformatics analyses revealed its potential to regulate E2 synthesis in sow GCs [30]. The aim of this study was to investigate the role and underlying mechanism of NORFA in the regulation of E2 synthesis. Through multidimensional analyses, we clarified that NORFA promoted E2 synthesis and inhibited sow GC apoptosis through a novel axis consisting of steroidogenic factor 1 (SF-1) and *cytochrome P450 family 11 subfamily A member 1 (CYP11A1)*. SF-1, encoded by *NR5A1*, is essential for the steroidogenesis in mammals. While, *CYP11A1* is the coding gene of P450SCC which is the first-step rate-limiting enzyme for E2 synthesis [31]. Our findings demonstrate that NORFA, as a pluripotent lncRNA, is crucial for E2 synthesis, follicular development and sow fertility.

Materials and methods

Animal and ethics

In this study, a total of 185 healthy, sexually-mature Duroc×Landrace×Yorkshire sows in the diestrus period (average 180 days and 110 kg mass) were randomly selected from Zhushun Biotechnology Co., Ltd (Nanjing, China) for ovaries collection, follicle isolation, and GC culture in vitro. The sows were fed, taken care, and slaughtered in accordance with the Regulations for the Administration of Affairs Concerning Experimental Animals (No.2 of the State Science and Technology Commission, 11/14/1988). All the animal-related experiments involved in this study were reviewed, approved, and supervised by the Animal Ethics Committee of Nanjing Agricultural University (NJAU.No20220324059).

Bioinformatics analysis

The RNA-seq datasets for NORFA knockdown in sow GCs were uploaded to NCBI SRA database (Bioproject

ID: PRJNA632987). Gene Set Enrichment Analysis (GSEA) was performed to identify the potential functions of NORFA-mediated DE mRNAs. miRNAs that potentially target *NORFA* and *CYP11A1* were predicted using four online programs: TargetScan v7.2, miRDB, miRWalk v3.0 database, and miRanda. The minimum free energy (MFE) of the interaction between miRNAs and target RNAs was analyzed using RNAhybrid. The promoters of pig *NR5A1* and *CYP11A1* were predicted using Promoter 2.0 and BDGP-NNPP. Transcription factors (TF) potentially bind to the *CYP11A1* promoter were analyzed by JASPAR database. The interaction between NORFA and *CYP11A1* promoter was predicted by Triplexator

and HNADOCK. The interaction between NORFA and *CYP11A1* mRNA was analyzed using LncTar and IntaRNA 2.0. catRAPID was utilized to analyze the interaction between NORFA and SF-1. The secondary structure of NORFA was analyzed using Mfold. The web addresses of the aforementioned tools are listed in Supplementary Table 1.

Follicle isolation and classification

The healthy antral follicles (HFs) and atretic antral follicles (AFs) were isolated from pig ovaries and classified according to the morphological identification, GC density, and estradiol/progesterone (E2/P4) ratio (Fig. 1C). In brief, HFs were recognized with red color

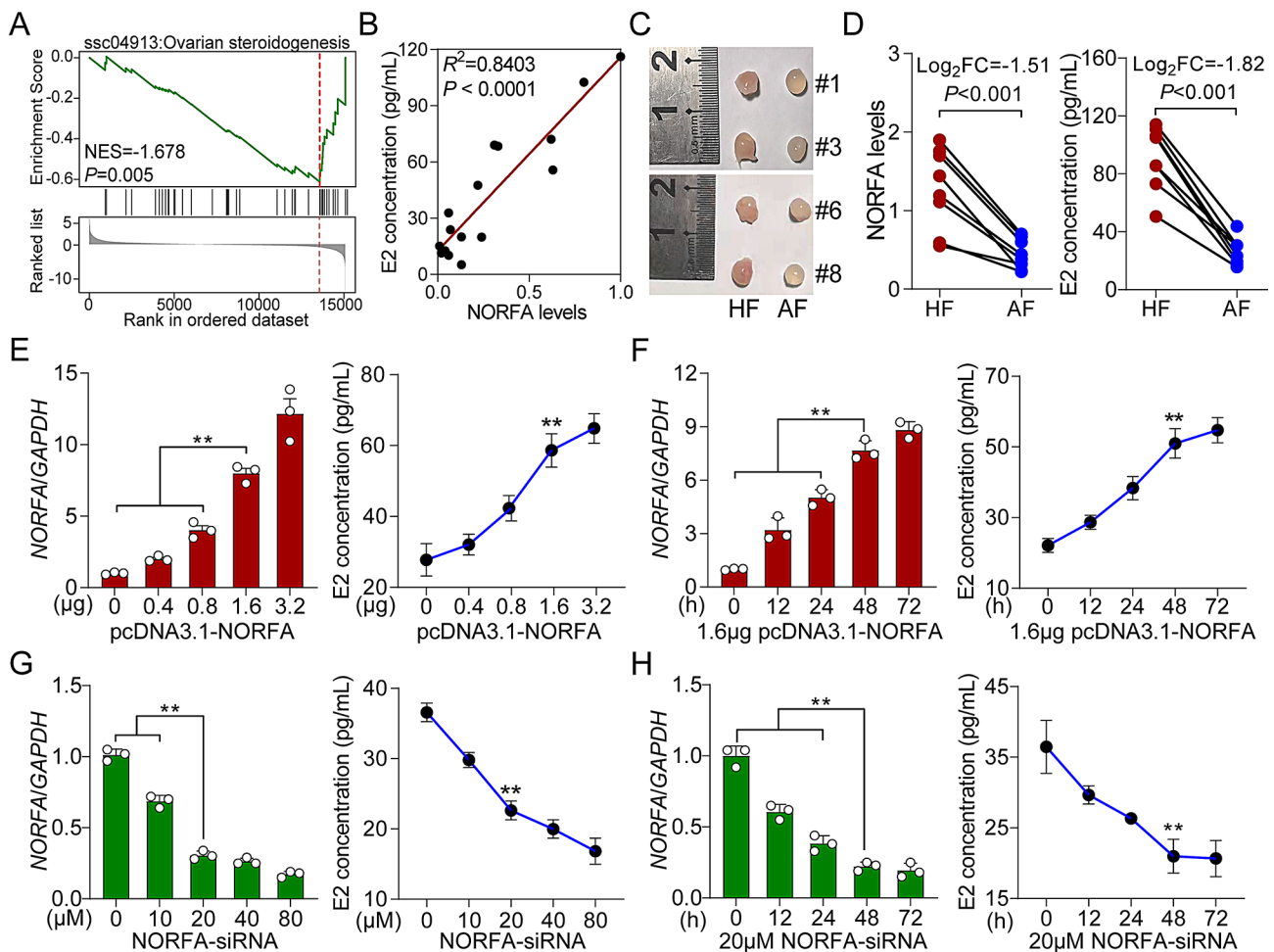


Fig. 1 NORFA is a novel inducer of E2 in sow GCs. **(A)** GSEA analysis based on RNA-seq data of NORFA knockdown showing a significant enrichment of the ovarian steroidogenesis pathway. **(B)** A significant positive correlation between the expression level of NORFA in the whole follicle and E2 levels in follicular fluid was identified by Pearson correlation analysis ($n = 16$). **(C)** Images of the healthy follicles (HF) and paired adjacent atretic follicles (AF) (paired $n = 8$). **(D)** Alteration patterns of NORFA expression (left) and E2 levels (right) in the HFs and AFs were detected using RT-qPCR and ELISA (paired $n = 8$). **(E)** NORFA expression (left) and E2 levels (right) in GCs transfected with pcDNA3.1-NORFA (0, 0.4, 0.8, 1.6 and 3.2 μg) for 48 h were detected using RT-qPCR and ELISA ($n = 3$). **(F)** After transfection with 1.6 μg pcDNA3.1-NORFA into GCs for different times (0, 12, 24, 48 and 72 h), NORFA expression (left) and E2 levels (right) were measured using RT-qPCR and ELISA ($n = 3$). **(G)** NORFA expression (left) and E2 levels (right) in GCs transfected with NORFA-siRNA (0, 10, 20, 40 and 80 μM) for 48 h were detected using RT-qPCR and ELISA ($n = 3$). **(H)** GCs were transfected with 20 μM NORFA-siRNA for the indicated times (0, 12, 24, 48 and 72 h), RT-qPCR and ELISA were performed to measure NORFA expression (left) and E2 levels (right) ($n = 3$). Data in **(E-H)** were shown as mean \pm SEM. Significance was analyzed by two-tailed Student's *t*-test and ANOVA. $**P < 0.01$

having blood vessels, low discrete GC density ($<2500/\mu\text{L}$), and a high E2/P4 ratio (>2.0). Only the follicles with morphology in accordance with the discrete GC density and E2/P4 ratio were selected for further investigation. The detailed numerical data about the GC density and E2/P4 ratio of eight paired HF and AFs are listed in Supplementary Table 2.

Cell culture and treatment

Sow GCs were isolated from 3 to 5 mm diameter healthy ovarian follicles using a 22-gauge needle and cultured in DMEM/F12 medium supplemented with 10% FBS and 1% penicillin-streptomycin. For transfection, GCs were seeded into 6- or 12-well plates and Lipofectamine™ 3000 Transfection Reagent (#L300015, Life Technologies) was utilized for oligonucleotides or plasmids transfection based on the manufacturer's instruction. The oligonucleotides utilized here (NORFA-siRNA, CYP11A1-siRNA, and StAR-siRNA) were synthesized by GenePharma (Shanghai, China) and listed in Supplementary Table 3. For cell treatment, the medium was replaced with FBS-free medium and cultured for 12 h. Then, ONO-2952 (#HY-111191, MCE), an effective inhibitor of the translocator protein (TSPO) which is necessary for the transport of CHOL into the inner mitochondrial membrane, was dissolved in DMSO and added to the medium at a final concentration of 10 μM .

RT-qPCR

Total RNA from ovarian follicles ($n=16$) and GCs was extracted using TRIzol reagent (#15596018, Invitrogen) and purified with the chloroform-isopropanol method. After detection of quality, quantity, integrity, and contamination, 1 μg total RNA was reverse-transcribed into cDNA using HiScript III RT SuperMix (#R323-02, Vazyme Biotech Co., Ltd.). qPCR reactions were conducted using AceQ qPCR SYBR Green Master Mix (#Q111-03, Vazyme Biotech Co., Ltd) on a QuantStudio 7 Flex system (Applied Biosystem) with three independent biological replicates. Expression levels of interested genes were calculated using the $2^{-\Delta\Delta\text{Ct}}$ method with normalization to *GAPDH*. The primers are presented in Supplementary Table 4.

Western blotting

Western blotting was performed following a standard protocol as previously described [32]. Briefly, total protein was extracted from sow GCs using cold RIPA lysis buffer (#P0013, Beyotime), and the concentration was measured with BCA method (#BL521A, Biosharp). A total of 15 μg protein was loaded and separated on 10% SDS-PAGE (#M00656, Genecrypt) and transferred to PVDF membranes (#IPFL00010, Millipore). The

membranes were blocked in 5% skim milk at room temperature for 2 h and incubated with primary antibodies at 4 °C overnight, followed by rinsed in the HRP-conjugated secondary antibodies at room temperature for 1 h. The membranes were visualized and the high-resolution original images were obtained by ChemiDoc densitometer with high-sensitivity ECL detection system (#E412, Vazyme Biotech Co., Ltd), which were quantified using ImageJ software. Primary antibodies used here were anti-P450SCC (#D122183, Sangon, rabbit, 1:1000), anti-SF-1 (#18658-1-AP, Proteintech, rabbit, 1:1000), and anti-GAPDH (#TA802519, ORIGENE, mouse, 1:3000).

Chromatin immunoprecipitation (ChIP)

ChIP was performed to detect the enrichment of SF-1 on the promoter of *CYP11A1* in sow GCs as previously described [33]. In brief, GCs were crosslinked using 1% formaldehyde for 10 min and quenched with 5 M glycine. Then, SF-1/DNA complexes were pulled down with the anti-SF-1 antibody (#18658-1-AP, Proteintech, rabbit). After ultrasonication, decrosslinking and purification, SF-1-interacted DNA fragments and their enrichment were identified and quantified by PCR and qPCR. Anti-IgG antibody (#sc2358, Santa Cruz Biotechnology, mouse) was used as negative control, and 10-fold diluted unprocessed chromatin served as input. The primers are presented in Supplementary Table 4.

RNA immunoprecipitation (RIP)

GCs were crosslinked with 1% formaldehyde and incubated with RIP lysis buffer at 4 °C for 30 min. After centrifuged at 13,000 rpm for 20 min, the supernatant was precleared and incubated with 4 μg anti-SF-1 antibody and 100 μL Protein A dynabeads (#10008D, Invitrogen) at 4 °C for 3 h. Beads were washed with RIP lysis buffer four times at 4 °C for 5 min and decrosslinked at 70 °C for 45 min. Finally, RNA was extracted using TRIzol reagent, and further identified and quantified using RT-qPCR analysis.

Biotinylated RNA pull-down

The single-stranded RNA transcripts of NORFA were transcribed in vitro, biotinylated using the Biotin RNA Labeling Mix (#11685597910, Roche) and T7 RNA polymerase (#EP0111, ThermoFisher Scientific), and purified with an RNeasy Mini Kit (#74104, Qiagen). 20 μg purified biotinylated transcripts were incubated with 60 μg total RNA or 100 μg total protein from sow GCs at room temperature for 4 h. Then, the biotin-RNA/RNA and biotin-RNA/protein complexes were pulled down with streptavidin magnetic beads (#LSKMAGT02, Merck Millipore). After isolation, the interacted RNAs and proteins were detected and quantified by RT-qPCR and western

blotting. To identify the specific interaction region of NORFA with NR5A1 mRNA and SF-1 protein, different truncated NORFA fragments were constructed.

RNA fluorescence in situ hybridization (RNA FISH)

RNA FISH was performed to detect the co-location of NORFA and NR5A1 mRNA in sow GCs. Briefly, cells were rinsed ephemerally in cold PBS and fixed with 4% formaldehyde for 20 min at room temperature. Then, cells were permeabilized in PBS with 0.5% Triton X-100 on ice for 5 min, and hybridization was performed using the following anti-sense probes: 5'-CGC GTT AGG GAC TGC CGC TTT CAG AGG ATT-3' for NORFA (green), and 5'-GTC AGC ACG CAC GGC TTC CAG GCG CAT C-3' for NR5A1 mRNA (red). Nuclei was stained with 4',6-diamidino-2-phenylindole (DAPI, blue). High-resolution images were obtained from an confocal laser scanning microscope (LSM 900, Zeiss) at 550 nm wavelength.

Immunofluorescence (IF)

Sow GCs seeded on the coverslips for IF were fixed with 4% paraformaldehyde, permeabilized with 0.1% Triton X-100, blocked with BSA, and incubated with rabbit anti-SF-1 antibody (#18658-1-AP, Proteintech, 1:200) overnight at 4 °C. After washed with TBST three times, GCs were then incubated with the CY3 590-conjugated goat anti-rabbit IgG (H+L) secondary antibody (#1111213-96, ImmunoReagents) for 1 h at room temperature. Meanwhile, DAPI (#C1006, Beyotime) was applied to stain the nuclei of sow GCs. Finally, representative high-resolution images were obtained from an fluorescence microscopy equipped with a Nikon DS-2 digital camera at 590 nm wavelength.

PREG and E2 detection

The concentrations of pregnenolone (PREG) and E2 in the GC culture medium and in the follicular fluid (FF) of healthy and atretic follicles were measured using a Pregnenolone Detection Kit (#MM-7789501, MMBIO) and an Estradiol Detection Kit (#ARE-8800, BNIBT). In brief, the FF and GC culture medium after transfection for 48 h were collected and centrifuged at 3,000 g for 20 min at 4 °C. The supernatant was collected, 10-fold diluted, and transferred into an ELISA plates for 30 min at 37 °C. Then, 50 µL enzyme reagent, 100 µL developer, and 50 µL reaction termination buffer were successively added into the plate and incubated in a dark room for 30 min at 37 °C. Finally, the optical density of each sample was detected under 450 nm wavelength and converted to the concentrations of PREG and E2.

Plasmids construction and luciferase activity assay

To construct the overexpression plasmid, the full-length coding sequence of pig *NR5A1* was amplified and cloned

into the pcDNA3.1 vector (#V790, Invitrogen) between the *KpnI* and *XhoI* enzyme sites. The specific amplification primers were as follows: F, 5'-CTA GCT AGC ATG GAC TAT TGG TAC GAC GA-3' and R, 5'-GCT CTA GAA ATG AGC AGG TTG TTT CG-3'. To generate the luciferase reporters, the fragments of *CYP11A1* and *NR5A1* promoter were synthesized and cloned into pGL3-Basic vector (#1471, Promega) between the *KpnI* and *XhoI* enzyme sites, while the 3'-UTR of *CYP11A1* and *NR5A1* were amplified and cloned into pmirGLO vector (#E1330, Promega) between *NheI* and *XhoI* enzyme sites. The mutant plasmids were constructed using a SoSoo cloning kit (#1111, Tsingke) following the kit's manual. All the recombinant vectors were verified by Sanger sequencing. For luciferase activity assay, cells were harvested after transfection for 24 h, and the luciferase activities of *firefly* and *Renilla* were measured using a Dual-Luciferase Reporter Assay System (#E1910, Promega). Relative luciferase activity of each sample was considered as the activity of *firefly* luciferase relative to *Renilla* luciferase.

Proliferation analysis

The proliferation of sow GCs was analyzed by Cell Counting Kit-8 (CCK-8) and 5-ethynyl-2'-deoxyuridine (EdU) assays. For CCK-8 assay, cells were seeded into 96-well plate with a density of 2,000 cells per well. After treatment for 24 h, 10 µL CCK-8 reagent (#FC101, Transgen) was added into the culture medium and incubated in a 37 °C dark room for 2 h. Then, the absorbance of each sample was measured under the optical density of 450 nm. EdU assay was performed using the BeyoClick™ EdU-488 Cell Proliferation Detection Kit (#K1076, APEx-BIO). Briefly, after labeling, fixation, and nuclei staining, the red fluorescence in GCs was observed under a fluorescence laser confocal microscope (ZEISS) at 488 nm wavelengths.

Apoptosis detection

GC apoptosis under different conditions was detected using an Annexin V-FITC/PI Apoptosis Detection kit (#A211, Vazyme Biotech Co., Ltd). Briefly, 20,000 cells were collected and dyed with 3 µL annexin V-FITC and 3 µL Propylidide (PI) at in a dark room for 15 min, and further sorted by flow cytometry on a cell counting system (#FACSScalibur, BD). Cell apoptosis rate was analyzed using Flowjo software, which was calculated based on the percentage of cells in Q2 (early apoptosis) and Q3 (late apoptosis) quadrants. Besides, the expression levels of apoptosis-related genes (*BCL2*, *BAX* and *Caspase3*) in GCs were detected by RT-qPCR and the *BCL2/BAX* ratio was statistically analyzed. The primers used here are listed in Supplementary Table 4.

ActD chase assays

ActD chase assays were conducted following the method as previously described [34]. In brief, actinomycin D (ActD; #A4262, Sigma), a general transcription inhibitor, was added to the medium at a final concentration of 5 µg/mL for the indicated times after transfection for 12 h. Total RNA was isolated and the mRNA levels of CYP11A1, NR5A1 and Luciferase were detected using RT-qPCR and compared to their levels at 0 h. Half-life times ($t_{1/2}$) were calculated by fitting multiple exponential mathematical models (nonlinear regression analysis) for mRNA levels across different time points.

Statistical analysis

Data in this study were presented as mean ± standard error (SEM) with at least three independent biological replicates. Pearson correlation analyses were performed by GraphPad Prism v8.0. Significance between two groups and three or more groups were calculated by IBM SPSS Statistics v26.0 with two-tailed Student's *t*-test and ANOVA. Statistical significance were labeled as **P* < 0.05 and ***P* < 0.01 for significant and extremely significant, respectively. The graphs were generated using GraphPad Prism v8.0 and RStudio v3.5.1.

Results

NORFA induces E2 synthesis in sow GCs

Based on the RNA-seq data (NORFA knockdown) and GSEA analysis, we found a significant enrichment of the ovarian steroidogenesis pathway, and most of the genes in this pathway were downregulated in sow GCs after NORFA knockdown (Fig. 1A). Interestingly, a significant positive correlation between the expression level of NORFA in whole follicle and E2 concentration in the follicular fluid was identified by Pearson correlation analysis (Fig. 1B), and both of which were dramatically downregulated during follicular atresia with similar alteration patterns (Fig. 1C-D), suggesting that NORFA is involved in the regulation of E2 synthesis. To address this, we subsequently investigated with gain-or-loss of function in sow GCs cultured in vitro and revealed that overexpression of NORFA significantly induced E2 synthesis in a dose- and time-dependent manner (Fig. 1E-F), whereas the opposite results occurred after knockdown of NORFA (Fig. 1G-H). These findings demonstrate that NORFA is a novel inducer of E2 synthesis in sow GCs.

NORFA promotes the synthesis of PREG in sow GCs

To analyze the mechanism by which NORFA induces E2 synthesis in sow GCs, we first examined the effect of NORFA on pregnenolone (PREG) synthesis, since the conversion of CHOL into PREG by entering mitochondria is the first key rate-limiting step of E2 synthesis. ELISA was performed and showed that overexpression

of NORFA significantly increased the PREG level in sow GCs, while the opposite results were observed after NORFA inhibition, both in a dose- and time-dependent manner (Fig. 2A-D). Besides, a significant positive correlation between the expression level of NORFA in follicles and the concentrations of PREG in follicular fluids, as well as similar alteration patterns during follicular atresia were identified by Pearson correlation and comparative analyses (Fig. 2E-F). Furthermore, we also noticed that the promotion of PREG by NORFA was seriously impaired by blocking CHOL transport into mitochondria through TSPO inhibitor (ONO-2952) addition or StAR-siRNA transfection (Fig. 2G-H). The above findings indicate that NORFA promotes the synthesis of PREG, which further induces E2 synthesis in sow GCs.

CYP11A1 is a positive functional target of NORFA

To clarify the regulatory mechanism of NORFA to PREG, an in-depth analysis based on RNA-seq data was performed and found that nine steroidogenesis-related genes were significantly downregulated after knockdown of endogenous NORFA, including *CYP11A1* (Fig. 3A-B). Since P450SCC is a rate-limiting enzyme for PREG synthesis, we hypothesized that NORFA promotes PREG synthesis by inducing the expression of its coding gene *CYP11A1*. Pearson correlation analysis revealed a significant positive correlation between NORFA and *CYP11A1* mRNA levels (Fig. 3C), and the expression level of *CYP11A1* was dramatically downregulated during follicular atresia (Fig. 3D), which is similar to the alteration pattern of NORFA. Quantitative assays showed that both mRNA and protein levels of *CYP11A1* were dramatically decreased in NORFA-silenced sow GCs, whereas the converse results occurred after NORFA overexpression (Fig. 3E-F), indicating that NORFA induces *CYP11A1* expression in sow GCs. To further analyze whether *CYP11A1* is a functional target of NORFA, a series of experiments based on *CYP11A1*-siRNA were conducted and we found that knockdown of *CYP11A1* disrupted the promotion of PREG and E2 synthesis by NORFA, as well as its pro-proliferative function in sow GCs (Fig. 3G-K, Supplementary Fig. 1). Taken together, these results demonstrate that *CYP11A1* is a positive functional target of NORFA in sow GCs.

SF-1 induces CYP11A1 transcription by acting as a transcription activator

Our previous study has confirmed that NORFA can sponge miRNAs by acting as a ceRNA in sow GCs. Therefore, we wondered whether NORFA regulated *CYP11A1* expression in the same way. However, we did not identify any miRNA that potentially mediates the regulation based on bioinformatic analyses and RNA-seq data (Fig. 4A-B). Besides, it was noticed that neither

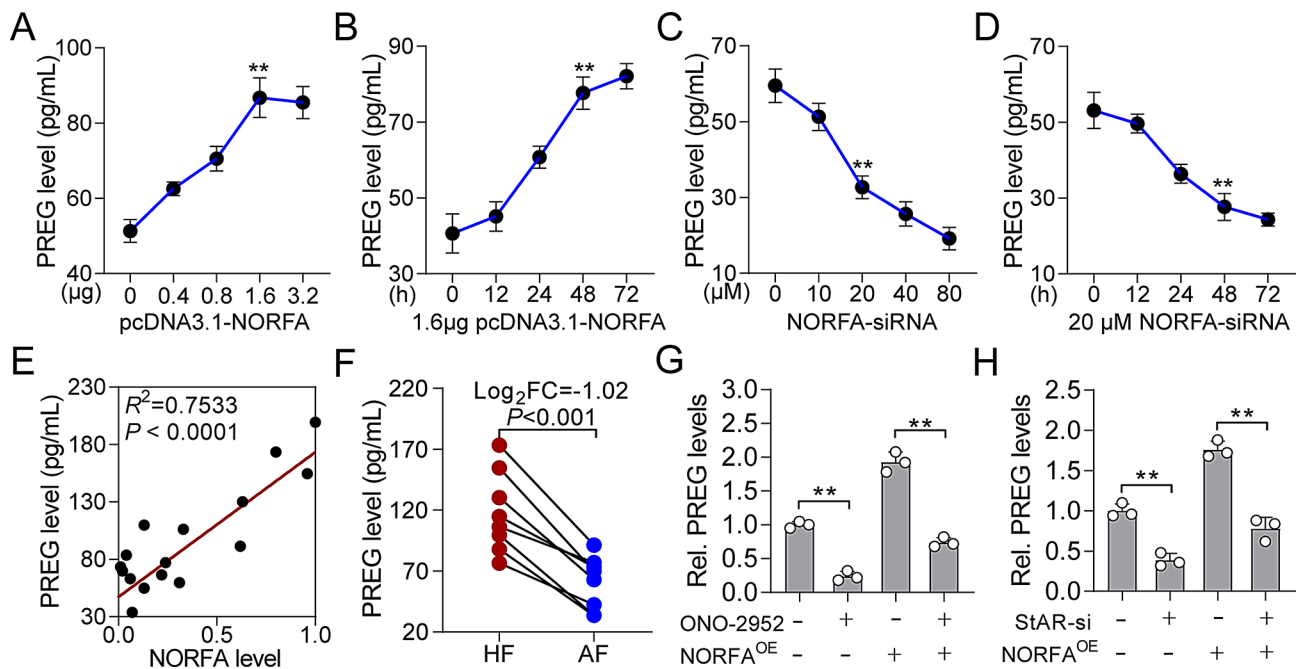


Fig. 2 NORFA induces the synthesis of PREG in sow GCs. **(A)** The levels of PREG in GCs transfected with indicated amount of pcDNA3.1-NORFA (0, 0.4, 0.8, 1.6 and 3.2 μg) for 48 h were detected by ELISA ($n=3$). **(B)** 1.6 μg pcDNA3.1-NORFA was transfected into GCs for different times (0, 12, 24, 48 and 72 h), and PREG levels were measured by ELISA ($n=3$). **(C)** PREG concentrations in GCs transfected with indicated amount of NORFA-siRNA (0, 10, 20, 40 and 80 μM) for 48 h were detected by ELISA ($n=3$). **(D)** 20 μM NORFA-siRNA was transfected into GCs for the indicated times (0, 12, 24, 48 and 72 h), ELISA was performed to measure PREG levels ($n=3$). **(E)** A significant positive correlation between NORFA expression in GCs and PREG levels in follicular fluid was identified by Pearson correlation analysis ($n=16$). **(F)** Alteration patterns of PREG levels in the HF and AFs were detected by ELISA (paired $n=8$). **(G-H)** The effects of NORFA overexpression (NORFA^{OE}) co-treated with 10 μM ONO-2952 (**G**) or 20 μM StAR-siRNA (**H**) on the PREG levels in GCs were detected by ELISA ($n=3$). Data were shown as mean \pm SEM with at least three independent replicates. Significance was analyzed by two-tailed Student's *t*-test and ANOVA. ** $P < 0.01$

the overexpression nor the knockdown of *NORFA* had a significant effect on the 3'-UTR activity of *CYP11A1* (Fig. 4C), indicating that miRNAs are not involved in the regulation of *NORFA* to *CYP11A1*. Recent studies have shown that cytoplasmic lncRNAs can directly bind to the target mRNAs and regulate their stability. Analyses of two algorithms (IntaRNA and LncTar) only found short interaction regions and low binding energy between *NORFA* and *CYP11A1* mRNA (Fig. 4D). Notably, the stability of *CYP11A1* mRNA remained unaffected in sow GCs after gain-or-loss function of *NORFA* (Fig. 4E). Collectively, these findings demonstrate that the regulation of *NORFA* to *CYP11A1* does not occur at the post-transcriptional level.

To next clarify whether *NORFA* induces *CYP11A1* expression at the transcription level, the promoter of *CYP11A1* was identified (Supplementary Fig. 2A), and we found that *NORFA* significantly promoted its transcription activity (Fig. 5A). Interestingly, SF-1, a transcription factor encoded by *NR5A1*, was considered to mediate the regulation of *NORFA* to *CYP11A1* through promoter character analysis and *NORFA*-mediated DETFs identification (Fig. 5B and Supplementary Fig. 2B). Quantitative analyses showed that

overexpression of *NR5A1* notably induced *CYP11A1* expression at both mRNA and protein levels (Fig. 5C-D), while a significant positive correlation was observed between the mRNA levels of *NR5A1* and *CYP11A1* in sow follicles (Fig. 5E). Luciferase activity detection showed that overexpression of *NR5A1* induced the activity of reporter vector containing *CYP11A1* promoter with wild-type SF-1 binding element (SBE), but had no effect on the vector with mutant SBE (Fig. 5F-G), indicating that SF-1 can recognize and bind to the SBE within *CYP11A1* promoter, which was further confirmed by ChIP assay (Fig. 5H). In addition, ELISA was conducted and revealed that SF-1 significantly facilitated the synthesis of PREG and E2, which was reversed by *CYP11A1* interference (Fig. 5I-K). Taken together, these results demonstrate that SF-1 induces *CYP11A1* transcription and E2 synthesis by acting as a transcription factor.

SF-1, induced by *NORFA* at the post-transcriptional level, mediates the regulation of *NORFA* to *CYP11A1*

RNA-seq data showed that *NR5A1* transcription level was downregulated in sow GCs after *NORFA* inhibition (Fig. 6A), while a significant positive

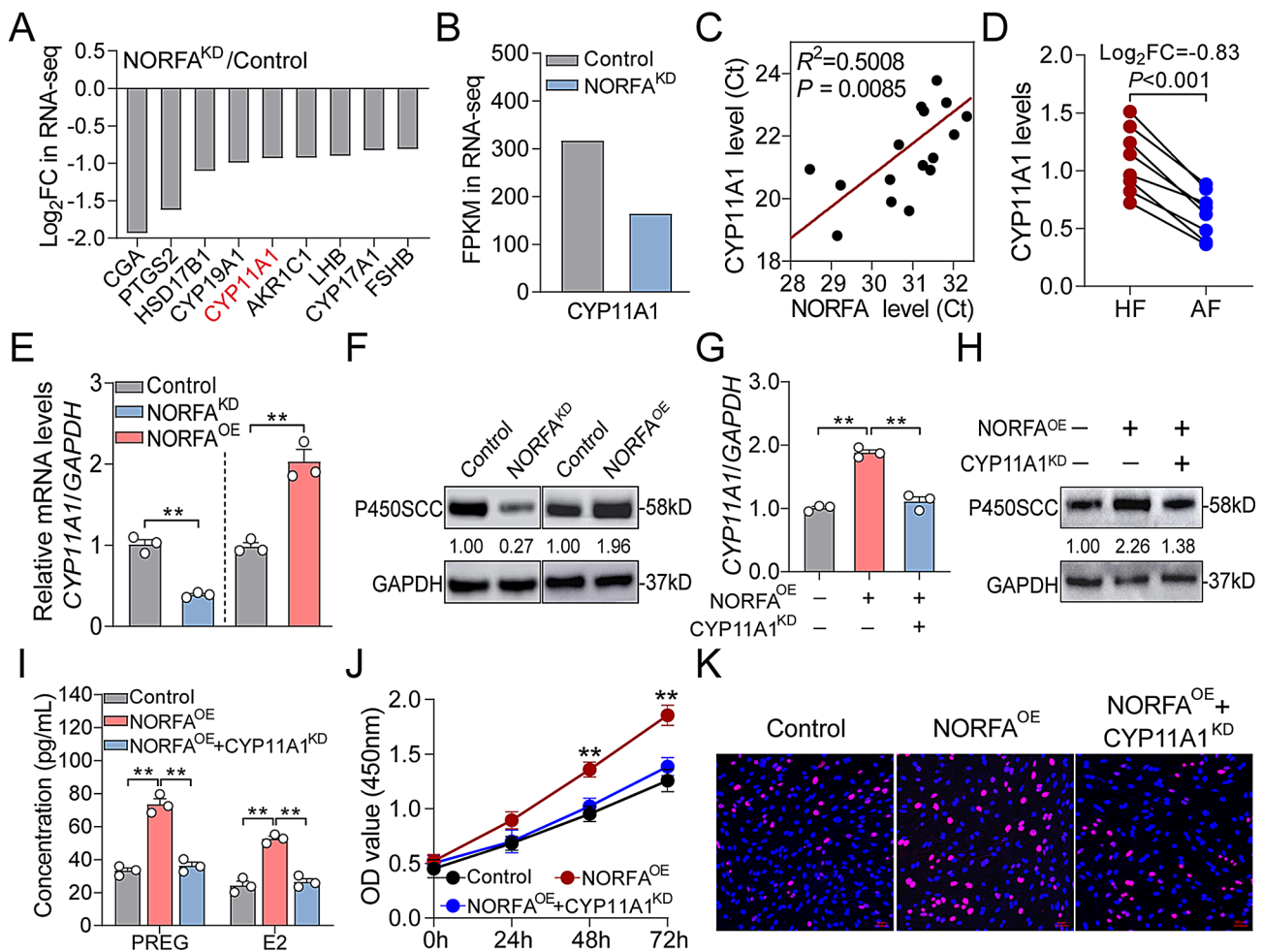


Fig. 3 *CYP11A1* is positively regulated by NORFA and mediates its function in sow GCs. **(A)** The expression patterns of nine steroid hormone synthesis-related genes in sow GCs after NORFA knockdown (NORFA^{KD}) were obtained from RNA-seq. **(B)** The FPKM values of *CYP11A1* mRNA in control and NORFA-inhibited sow GCs were obtained from RNA-seq. **(C)** The expression correlation between NORFA and *CYP11A1* mRNA in follicles was identified by Pearson correlation analysis ($n = 16$). **(D)** Alteration patterns of *CYP11A1* mRNA levels in the HF and AF follicles were detected by RT-qPCR (paired $n = 8$). **(E–F)** The effects of NORFA overexpression (NORFA^{OE}) or knockdown (NORFA^{KD}) on the mRNA **(E)** and protein **(F)** levels of *CYP11A1* in sow GCs were analyzed by RT-qPCR and western blotting ($n = 3$). **(G–K)** pcDNA3.1-NORFA (NORFA^{OE}) was co-transfected with *CYP11A1*-siRNA (*CYP11A1*^{KD}) into sow GCs for 48 h, the mRNA **(G)** and protein **(H)** levels of *CYP11A1* were detected by RT-qPCR and western blotting ($n = 3$), the concentration of PREG and E2 were measured using ELISA **(I)**, $n = 3$, and GC proliferation was analyzed by CCK-8 **(J)** and EdU staining **(K)**. Data were shown as mean \pm SEM with at least three independent replicates. Significance was analyzed by two-tailed Student's *t*-test and ANOVA. ** $P < 0.01$

correlation between NORFA and NR5A1 levels was identified (Fig. 6B), indicating that NORFA induces *NR5A1* expression, which was further confirmed by quantitative analyses (Fig. 6C–D). Bioinformatic analysis and luciferase activity detection revealed that the regulation of NORFA to *NR5A1* does not occur at transcriptional level (Supplementary Fig. 3). ActD chase assay was performed and found that knockdown of NORFA shortened the half-life time of *NR5A1* mRNA, which was prolonged by NORFA overexpression (Fig. 6E), indicating that NORFA stabilizes *NR5A1* mRNA at the post-transcriptional level. Interestingly, RNA-FISH showed that NORFA colocalized with *NR5A1* mRNA in the cytoplasm (Fig. 6F),

suggesting a direct interaction between them. Prediction by IntaRNA 2.0 found that NORFA potentially bind to the 3'-UTR of *NR5A1* mRNA through three interaction regions, termed as IR1 (156–200 nt), IR2 (509–558 nt), and IR3 (633–682 nt) (Supplementary Fig. 4A). Moreover, six biotinylated fragments of NORFA were constructed based on its secondary structure (Supplementary Fig. 4B), and RNA pull-down assays showed that full-length NORFA or fragment with IR1, but not IR1 deletions, could pull down *NR5A1* mRNA (Fig. 6G), indicating that IR1 is essential for NORFA to recognize and interact with *NR5A1* mRNA. Notably, NORFA with IR1 deletion lost the ability to stabilize *NR5A1* mRNA (Fig. 6H).

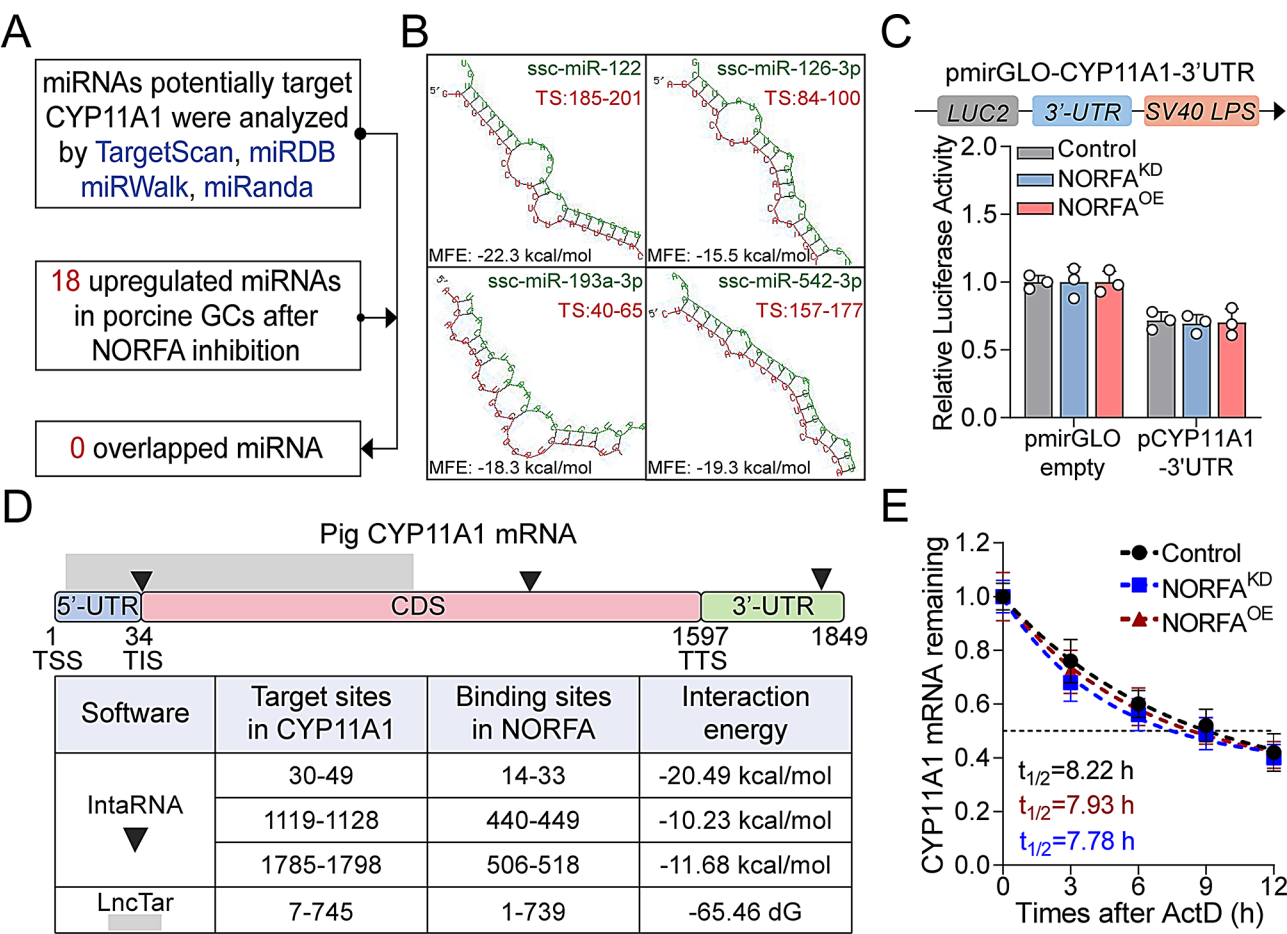


Fig. 4 The regulation of NORFA to *CYP11A1* dose not occur at post-transcriptional level. **(A)** No overlapped miRNA was found between miRNAs potential-ly targeting *CYP11A1* and NORFA-mediated DEmiRNAs. **(B)** Four NORFA-mediated DEmiRNAs were predicted targeting *CYP11A1* 3'-UTR with poor seed sequence paring and low minimum free energy (MFE) by RNAhybrid. TS indicates the target site on *CYP11A1* mRNA. **(C)** Effects of NORFA overexpression (NORFA^{OE}) or knockdown (NORFA^{KD}) on the 3'-UTR activities of *CYP11A1* were analyzed using luciferase activity assays (*n* = 3). **(D)** The interaction between NORFA and *CYP11A1* mRNA was analyzed using two algorithms (IntaRNA and LncTar), TSS was considered as +1. **(E)** Effects of NORFA overexpression (NORFA^{OE}) or knockdown (NORFA^{KD}) on the stability of *CYP11A1* mRNA were detected by ActD chase assays (*n* = 3). Data were shown as mean ± SEM with at least three independent replicates

Furthermore, quantitative analyses and ELISA showed that SF-1 partially restored the expression of *CYP11A1* and the synthesis of PREG and E2, which were inhibited by NORFA knockdown (Fig. 6I-K). These findings demonstrate that NORFA stabilizes NR5A1 mRNA by directly binding to its 3'-UTR, and SF-1 at least partially mediates the regulation of NORFA to *CYP11A1* expression and E2 synthesis.

NORFA tethers SF-1 to shuttle into nucleus in sow GCs

As shown in Fig. 6I and K, overexpression of SF-1 only partially restored the *CYP11A1* expression and E2 level in NORFA-inhibited sow GCs, suggesting the existence of additional regulatory mechanism between NORFA and SF-1. Notably, ChIP and IF detection showed that SF-1 overexpression was unable to fully restore its enrichment on the promoter of *CYP11A1*, and the novel synthesized SF-1 were predominantly

located in the cytoplasm of sow GCs under the condition of NORFA knockdown (Fig. 7A-B), indicating that NORFA is essential for the nucleus translocation of SF-1. Interestingly, colocalization analysis by FISH and IF revealed that NORFA and SF-1 colocalized in the cytoplasm and nucleus (Fig. 7C). To further validate their physical interaction, RIP was conducted and showed that SF-1 directly interact with NORFA in sow GCs (Fig. 7D). Moreover, three potential interaction regions (60–120 nt, 310–450 nt and 510–650 nt) of NORFA with SF-1 were predicted by catRAPID analysis (Fig. 7E). Five biotinylated NORFA fragments (FL: full-length; F1: 1-160 nt; F2: 161–299 nt; F3: 300–499 nt; F4: 500–739 nt) were constructed and RNA pull-down assays showed that F1, F3 and F4 fragments of NORFA were indispensable for its interaction with SF-1 (Fig. 7F). These findings demonstrate that

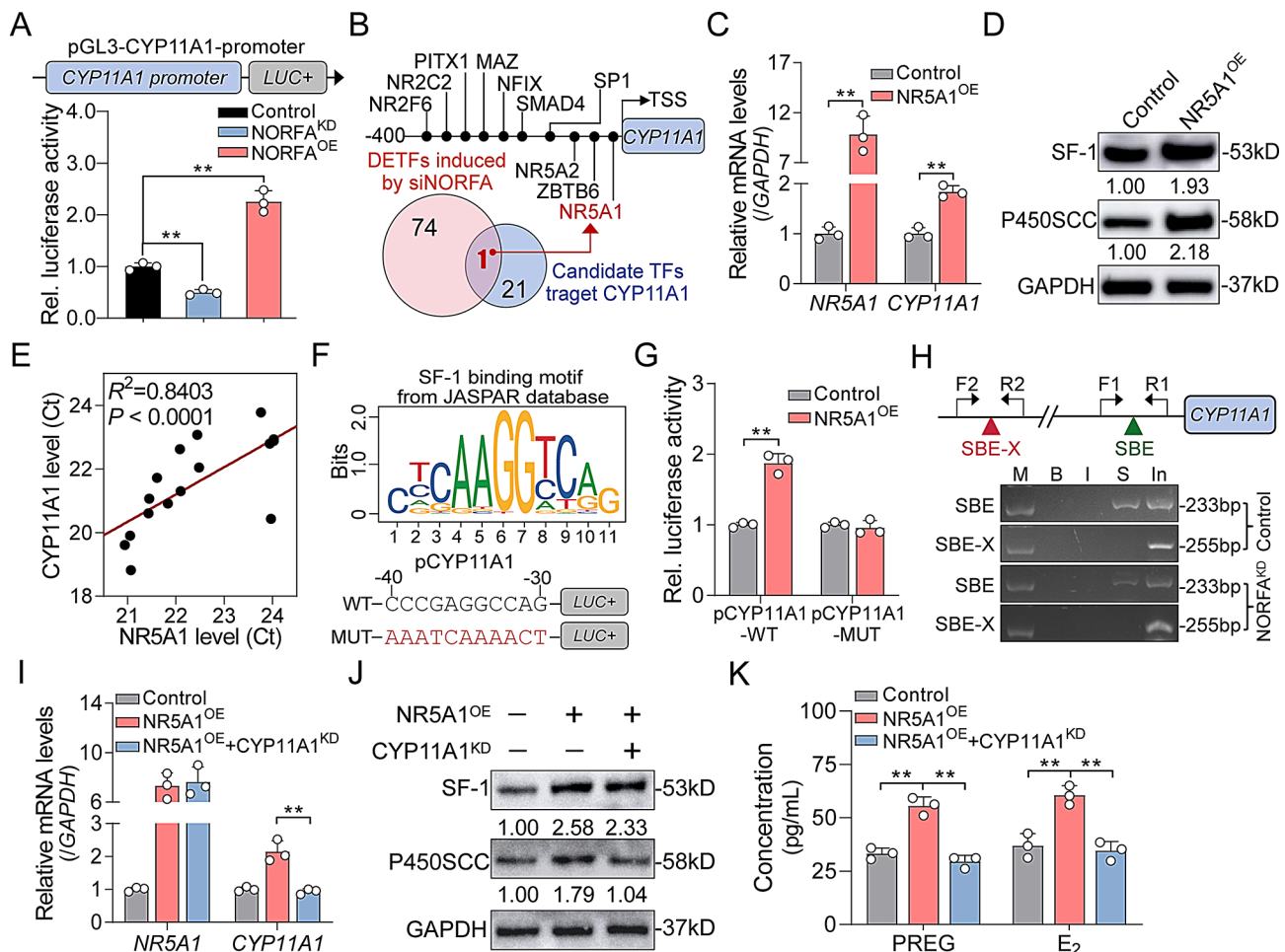


Fig. 5 SF-1, a transcriptional activator, induces *CYP11A1* transcription, PREG and E2 synthesis in sow GCs. **(A)** Effects of NORFA overexpression (NORFA^{OE}) or knockdown (NORFA^{KD}) on *CYP11A1* promoter activity were analyzed by luciferase activity assays ($n = 3$). **(B)** TFs that potentially target *CYP11A1* promoter were screened by JASPAR prediction and siNORFA-mediated DETFs obtained from previous RNA-seq data. **(C–D)** The mRNA and protein levels of *CYP11A1* in NR5A1 over-expressed sow GCs were detected using RT-qPCR and western blotting ($n = 3$). **(E)** The correlation between NR5A1 and *CYP11A1* mRNA levels was analyzed by Pearson correlation analysis ($n = 16$). **(F)** Diagram showing the reporter vector containing *CYP11A1* promoter with wild-type (WT) or mutant (MUT) SF-1 binding element (SBE). **(G)** Effects of NR5A1 overexpression (NR5A1^{OE}) on the activities of reporter vectors established in (F) were detected by luciferase activity assays ($n = 3$). **(H)** Enrichment of SF-1 on the promoter of *CYP11A1* in sow GCs transfected with or without siNORFA was analyzed by ChIP. F1/R1 and F2/R2 are the primer pairs for SBE and SBE-X (without SBE), respectively. M indicates DNA marker, B indicates blank, I indicates IgG, S indicates SF-1, In indicates input. **(I–K)** The expression of *CYP11A1* and the concentrations of PREG and E2 in sow GCs after co-transfection with pcDNA3.1-NR5A1 (NR5A1^{OE}) and *CYP11A1*-siRNA (*CYP11A1*^{KD}) were detected by RT-qPCR, western blotting, and ELISA ($n = 3$). Data were presented as mean \pm SEM with at least three independent replicates. Significance was analyzed by two-tailed Student's *t*-test and ANOVA. ** $P < 0.01$

NORFA tethers SF-1 and induces its nucleus translocation in sow GCs.

NORFA/SF-1/CYP11A1 axis inhibits the apoptosis and death of sow GCs

Previous studies have demonstrated that NORFA and E2 inhibit the apoptosis of sow GCs, which makes us wonder whether NORFA inhibits sow GC apoptosis through the SF-1/CYP11A1 axis. To address this, FACS assays were performed and showed that knockdown of *CYP11A1* significantly increased the apoptosis and death rate of sow GCs which was suppressed by the overexpression of NORFA or NR5A1 (Fig. 8A–B). Meanwhile,

overexpression of NR5A1 dramatically inhibited the apoptosis and death rate of sow GCs which was induced by NORFA knockdown (Fig. 8C). Besides, RT-qPCR was performed and showed that NORFA inhibited *Caspase3* expression and elevated the *BCL2/BAX* ratio in sow GCs through the SF-1/CYP11A1 axis (Fig. 8D–F). Taken together, these findings demonstrate that NORFA/SF-1/CYP11A1 axis plays an important role in inhibiting the apoptosis and death of sow GCs.

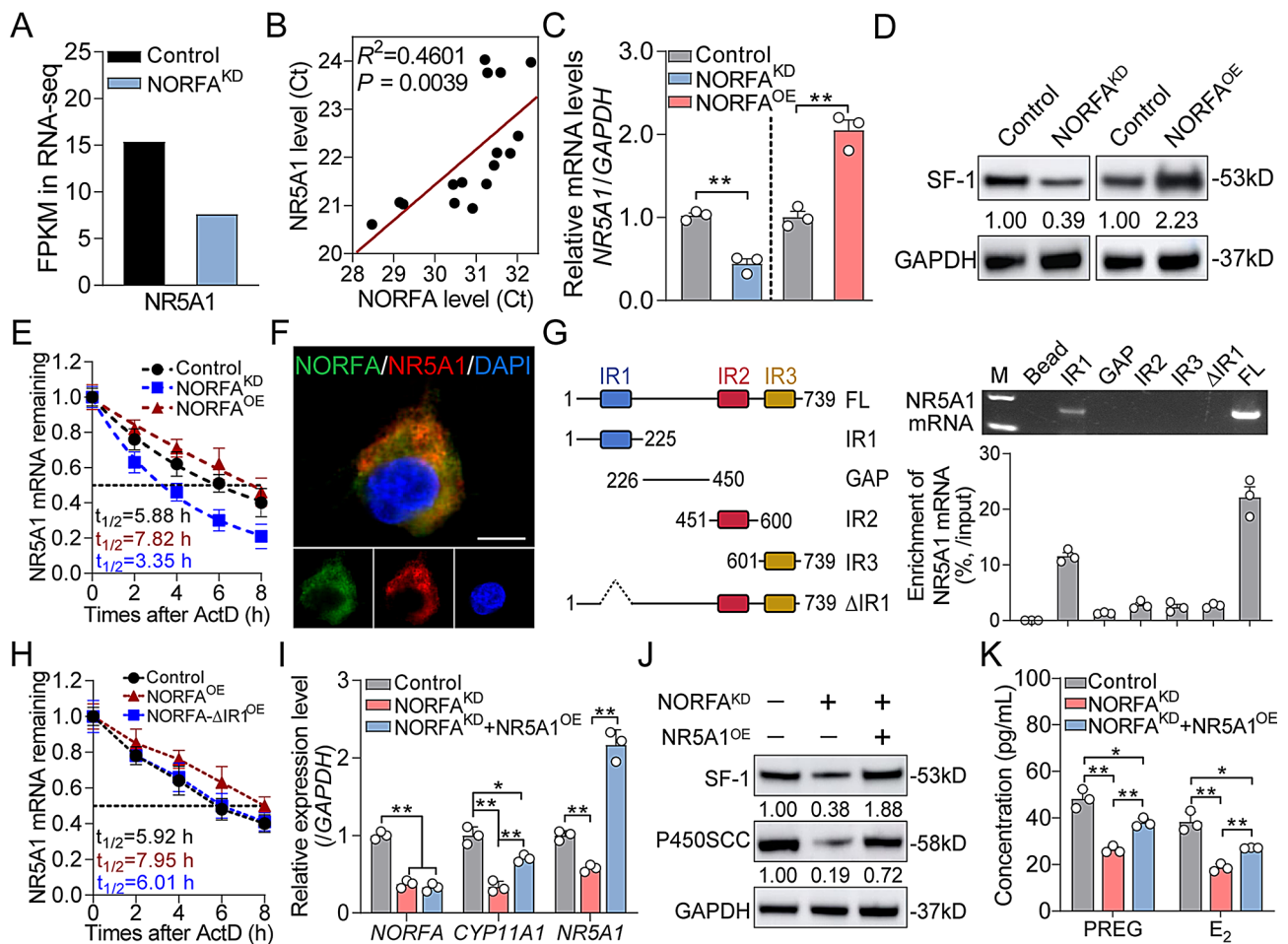


Fig. 6 SF-1, induced by NORFA at the post-transcriptional level, mediates the regulation of NORFA to *CYP11A1*. **(A)** The abundance of NR5A1 transcript in sow GCs after NORFA knockdown (NORFA^{KD}) was detected by RNA-seq. **(B)** Correlation between NORFA and NR5A1 expression levels was analyzed using Pearson correlation analysis ($n = 16$). **(C-D)** The effects of NORFA overexpression (NORFA^{OE}) or knockdown (NORFA^{KD}) on the mRNA **(C)** and protein **(D)** levels of NR5A1 in sow GCs were detected using RT-qPCR and western blotting ($n = 3$). **(E)** Effects of NORFA overexpression (NORFA^{OE}) or knockdown (NORFA^{KD}) on the stability of NR5A1 mRNA were analyzed using ActD chase assays ($n = 3$). **(F)** The colocalization of NORFA and NR5A1 mRNA in sow GCs was detected using RNA-FISH. Scale bar = 10 μ m. **(G)** Schematic view of truncated fragment of NORFA (left panel), and the physical interaction between NORFA and NR5A1 mRNA, as well as the interaction regions of NORFA were identified using RNA pull-down (right panel). **(H)** Effects of NORFA with IR1 deletion on the stability of NR5A1 mRNA were detected using ActD chase assays ($n = 3$). **(I-K)** The mRNA **(I)** and protein **(J)** levels of *CYP11A1*, PREG and E_2 concentration **(K)** in sow GCs after co-transfection with NORFA-siRNA (NORFA^{KD}) and pcDNA3.1-NR5A1 (NR5A1^{OE}) were detected by RT-qPCR, western blotting, and ELISA assays ($n = 3$). Data were presented as mean \pm SEM with three independent replicates. Significance was analyzed by two-tailed Student's *t*-test and ANOVA. * $P < 0.05$, ** $P < 0.01$

Discussion

Although huge amount of lncRNAs have been identified in livestock and poultry recently with the widespread application of high-throughput sequencing technology [35], most of which have not been functionally annotated. To our knowledge, only less than 400 functional lncRNAs were identified in domestic animals. Nevertheless, lncRNAs have been considered as key regulators of economic traits in livestock and poultry. For instance, MyH1-AS promotes the growth trait of chicken by inducing embryonic muscle development [36], TRT-MFS maintains the milk quality of cows by inducing fat synthesis in BMECs [37], H19 improves the wool trait

of goats by promoting the proliferation of DPs [38], and MREF increases the meat yield trait of pig by inducing myogenic differentiation and regeneration [39]. As another important economic trait, the reproductive trait of domestic animals was investigated recently and found it was also affected by lncRNAs. NORFA is the first validated sow fertility associated lncRNA, and is found to inhibit GC apoptosis and follicular atresia in our previous study [29], which is similar to the function of E2. However, the interaction between NORFA and E2 in sow GCs was unknown. This study demonstrates that NORFA is a novel inducer of E2 biosynthesis via the NR5A1/*CYP11A1* regulatory axis, which deepens the

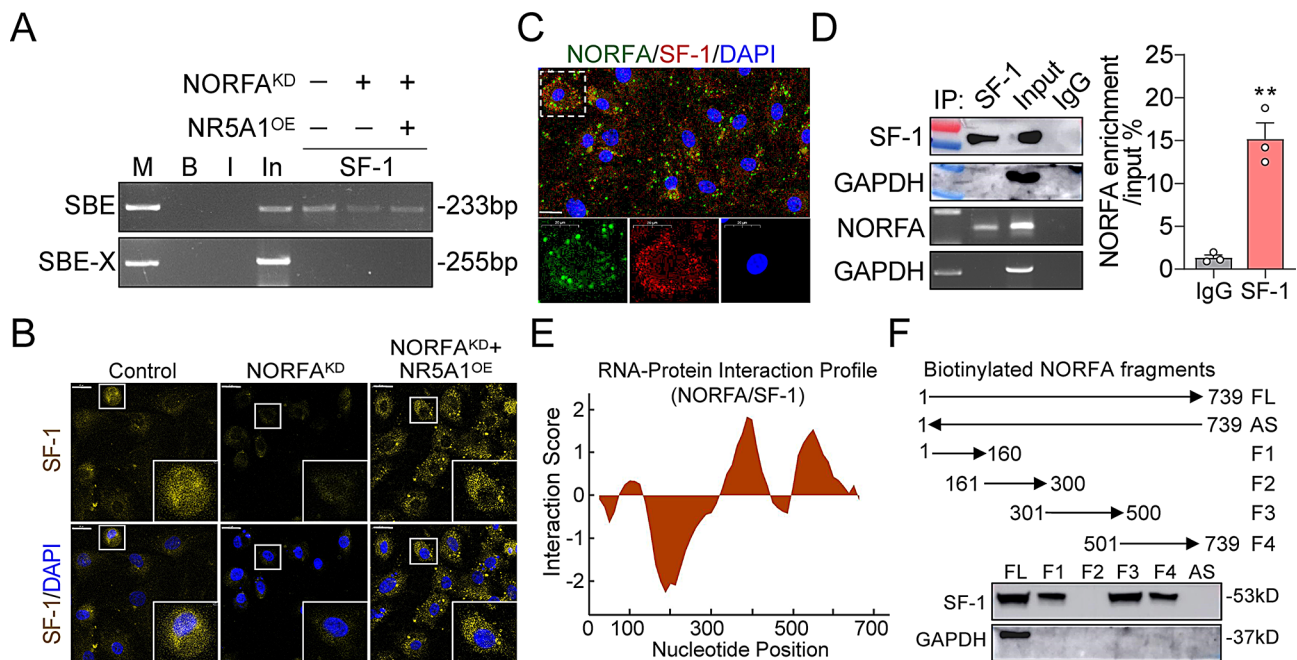


Fig. 7 NORFA tethers SF-1 to shuttle into nucleus. **(A)** The enrichment of SF-1 on the *CYP11A1* promoter under the indicated conditions was detected using ChIP. **(B)** The effects of NORFA knockdown (NORFA^{KD}) on the subcellular localization of SF-1 in sow GCs were analyzed using IF. Nuclei were stained with DAPI (blue). **(C)** FISH and IF were conducted to assess the co-localization between NORFA (green) and SF-1 (red) in sow GCs. **(D)** The physical interaction between NORFA and SF-1 was analyzed using RIP assay. Western blotting of SF-1 pull-downed by SF-1 antibody and RT-qPCR analysis of NORFA enriched by SF-1 protein in sow GCs were shown ($n=3$). IgG and GAPDH were served as negative and internal control, respectively. **(E)** The candidate interaction regions of NORFA with SF-1 were analyzed by catRAPID software. **(F)** Interaction regions of NORFA with SF-1 were identified using biotinylated RNA pull-down. Schematic diagram depicting the truncated fragments of NORFA (upper), and SF-1 protein pull-downed by the bioinylated NORFA fragments were detected using western blotting (lower). Data in **(D)** were presented as mean \pm SEM with three independent replicates. ** $P < 0.01$

understanding of functions of lncRNAs and expands the NORFA-mediated regulatory network in sow GCs.

Interactions between E2 and lncRNAs have been reported to be involved in the pathogenesis of multiple diseases in the ovary and other tissues, including PCOS, POE, endometriosis, breast cancer, thyroid cancer, and renal cell carcinoma. For example, a positive feedback regulatory loop formed between E2/ER β and H19 promotes thyroid carcinoma [40]. While, high level of TUG1 induces PCOS by inducing E2 synthesis [41]. However, only a few studies have investigated the interaction between E2 and lncRNAs in the ovaries of domestic animals, particularly in sow, and it is still unclear whether lncRNAs regulate the reproductive traits and fertility of sows by affecting E2 synthesis. Knapczyk et al. identified 23 DELncRNAs in the ovaries of piglets exposed to 4-tert-octylphenol (OP), a widely-used non-ionic surfactant to mimic E2 [42]. On the other hand, only three lncRNAs have recently been identified to regulate follicular development by affecting E2 synthesis in sows, but all through ceRNA mechanism. Specifically, nuclear NORSF reduces E2 release by sponging miR-339 in sow GCs [23], IFDD arrests follicular development by inhibiting E2 synthesis [27], while SFFD inhibits follicular atresia by promoting E2 synthesis [28]. In this study, NORFA was identified to

induce E2 in sow GCs through interacting with NR5A1 mRNA and SF-1 in ceRNA-independent manners, unlike the three aforementioned lncRNAs. Despite them, further studies are needed to in-depth investigate the interaction between E2 and lncRNAs in the ovaries of domestic animals, and more functional lncRNAs should be identified to reveal and expand the regulatory network of E2 synthesis.

P450SCC, encoded by *CYP11A1*, is located in the inner mitochondrial membrane and participates in a series of energy metabolism related biological processes [43]. Similar to other protein-coding genes, the transcription of *CYP11A1* is regulated by histone modification, DNA methylation, and TFs in multiple tissues among different species [44–46]. However, researches on the post-transcriptional regulation of *CYP11A1* are limited, and only 8 miRNAs and 4 lncRNAs with the ability to regulate *CYP11A1* expression have been reported to date. Among them, only miR-339 inhibits *CYP11A1* expression by directing binding to its 3'-UTR, and mediates the regulation of lnc-2300 to *CYP11A1* in sow GCs [47]. It is also noteworthy that other 7 miRNAs, such as miR-101-3p, regulate *CYP11A1* expression in an indirect manner [48], and the regulatory mechanism of 3 additional lncRNAs (SDNOR, Handos1, and lnc-SRA) remains unclear [49].

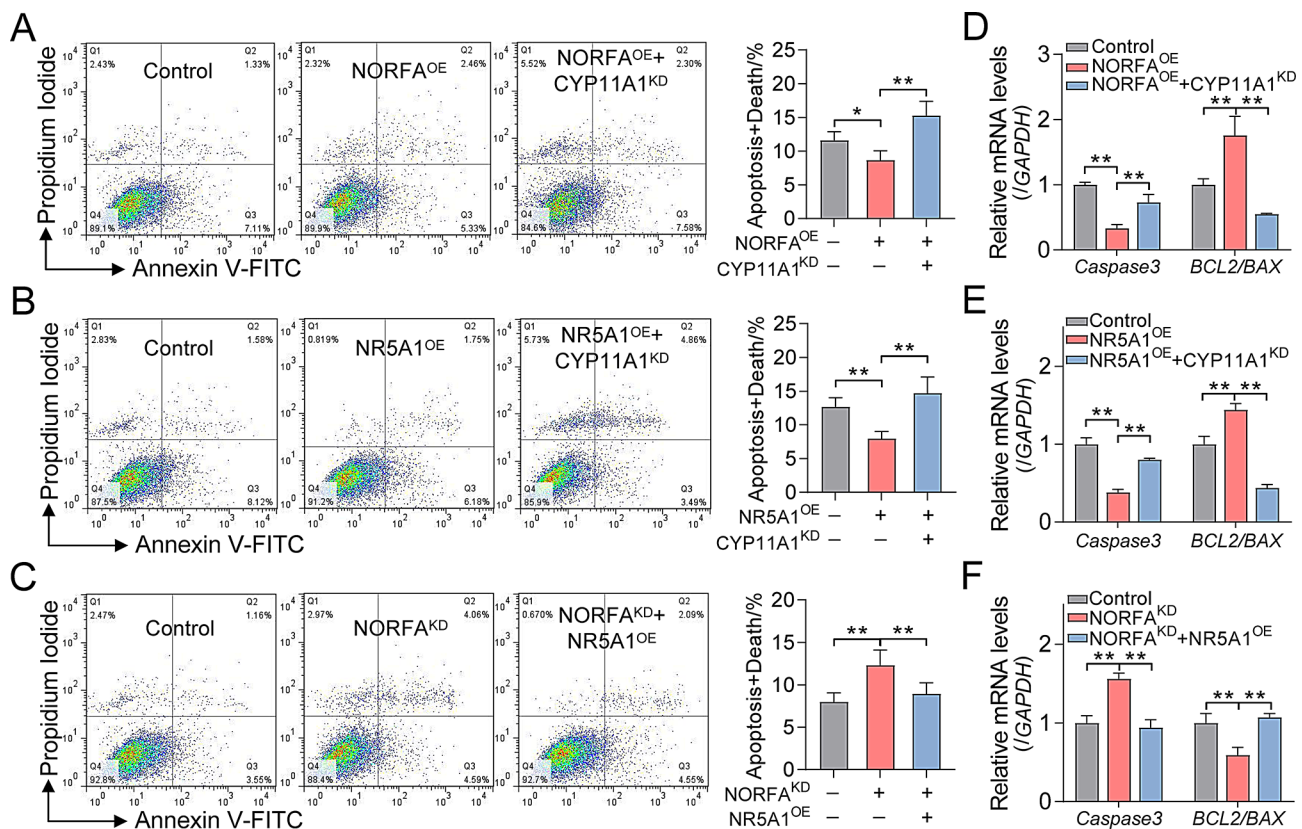


Fig. 8 NORFA/SF-1/CYP11A1 axis inhibits the apoptosis and death of sow GCs. (A–C) The apoptosis (Q2 + Q3) and death (Q4) rates of sow GCs after the indicated treatment were measured using FACS ($n=3$). (D–F) *Caspase3* expression levels and *BCL2/BAX* ratio in sow GCs under different conditions were detected by RT-qPCR analysis ($n=3$). Data are presented as mean \pm SEM with three independent replicates. Significance was analyzed by ANOVA. * $P < 0.05$, ** $P < 0.01$

Here, NORFA was identified as a novel lncRNA that induces *CYP11A1* expression in sow GCs through RNA-seq and quantitative analyses. It is well-known that the regulation mechanism of non-coding RNAs (miRNAs and lncRNAs) depends on their sub-cellular localization. NORFA is a nucleoplasmic lncRNA, indicating that it may function at different levels. Our findings showed that NORFA induces *CYP11A1* transcription through interacting with SF-1, rather than at the post-transcriptional level. To our knowledge, this is the first instance of a lncRNA interacting with TF to regulate E2 synthesis through affecting the expression of *CYP11A1*. Further investigations are required to validate whether it is a universal regulation mechanism for E2 synthesis in the ovaries among mammals.

Orphan nuclear receptors (ONRs) are a subset of nuclear receptor family with 25 members of TFs and co-regulators, which regulate fertility, metabolism, angiogenesis, immunity, and diseases by controlling the transcription of a wide range of target genes [50, 51]. Recent studies indicated that interactions between ONRs and lncRNAs are involved in multiple crucial biological processes. For example, NR2F1-AS1 induces lung

metastasis of breast cancer cells by promoting NR2F1 translation [52]. While, Nur77 activates the transcription of *WFDC21P* by acting as a TF, further attenuates the glycolysis-mediated HCC [53]. As one of the most important ONRs that is highly expressed in ovary and indispensable for steroidogenesis and mammalian reproduction, the interaction between SF-1 and lncRNAs is poorly known [54]. To date, only Hu et al. (2019, 2023) reported that lnc-Gm2044 promotes SF-1 expression by inducing the translation of NR5A1 mRNA in mouse GCs [55, 56]. However, whether and how lncRNAs regulate SF-1 expression in sow GCs has not yet been reported. In this study, we demonstrate that NORFA promotes SF-1 expression by stabilizing NR5A1 mRNA in sow GCs for the first time. In addition to the expression regulation, NORFA is also essential for SF-1 shuttling into nucleus to activate *CYP11A1* transcription, indicating that NORFA has the same canonical regulatory mechanism to the previously identified lncRNAs [57–59]. These findings reveal the regulation of lncRNA to SF-1, and elucidate the regulatory mechanism of lncRNA/TF axis to E2 synthesis in sow GCs. Further studies are needed to clarify

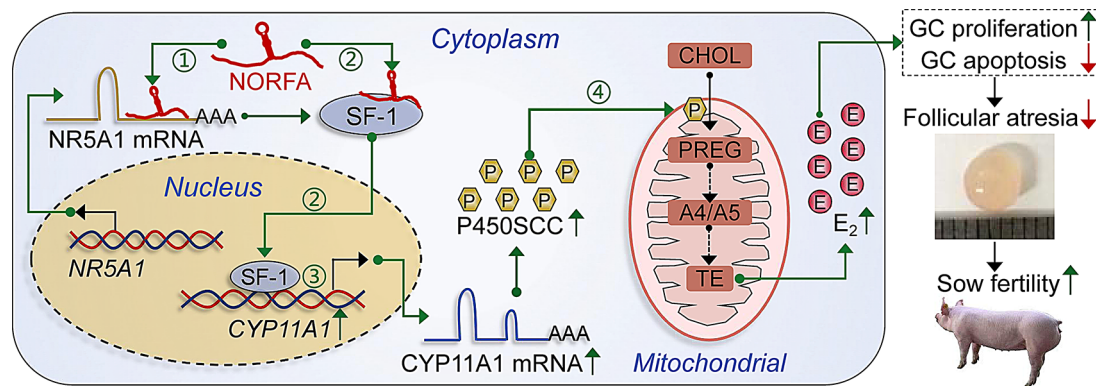


Fig. 9 A working model of the NORFA/SF-1/CYP11A1 regulatory axis in sow GCs. ① NORFA stabilizes NR5A1 mRNA by binding to its 3'-UTR. ② NORFA interacts with SF-1 and induces its nucleus transferring. ③ SF-1, as a transcription activator, induces *CYP11A1* transcription by binding to its promoter. ④ Up-regulation of P450SCC, encoded by *CYP11A1*, accelerates the conversion from CHOL to PREG, and induces the biosynthesis of E2, which further maintains the normal states of GCs and inhibits follicular atresia. A4 and A5 indicate androstenedione and androstenediol, respectively, which are the important intermediates of $\Delta 4$ and $\Delta 5$ pathway. TE indicates testosterone, which is the precursor of E2

the mechanism by which NORFA regulates the nuclear shuttling of SF-1.

Conclusion

In summary, we have investigated the epigenetic regulation of steroidogenesis in sow GCs and identified NORFA as a novel inducer of E2. NORFA promotes the expression of SF-1 at post-transcription level, and also induces the nucleus transfer of SF-1 to activate the transcription of *CYP11A1*, ultimately enhances E2 synthesis and inhibits GC apoptosis (Fig. 9). Our findings establish a bridge (SF-1/CYP11A1 axis) between NORFA and steroidogenesis, which contributes to further understanding of the regulatory mechanism of lncRNAs in reproductive system, and provides new clues for improving ovarian health and female fertility.

Abbreviations

CYP11A1	Cytochrome P450 family 11 subfamily A member 1
NORFA	Noncoding RNA involved in follicular atresia
SF-1	Steroidogenic factor 1
E2	17 β -estradiol
PREG	Pregnenolone
3'-UTR	3'-untranslated region
LncRNA	Long non-coding RNA
miRNA	MicroRNA
NR5A1	Nuclear receptor subfamily 5 group A member 1
TF	Transcription factor
SBE	SF-1 binding element
DElncRNAs	Differentially expressed lncRNAs

Supplementary Information

The online version contains supplementary material available at <https://doi.org/10.1186/s13062-024-00563-1>.

Supplementary Material 1: Figure S1. The knockdown efficiency of CYP11A1-siRNAs. Figure S2. Identification and characterization of the *CYP11A1* promoter. Figure S3. The regulation of NORFA to *NR5A1* does not occur at transcriptional level. Figure S4. NORFA potentially binds to the 3'-UTR of *NR5A1* mRNA. Table S1. The website addresses of online software and database. Table S2. The detailed numerical data of the eight pairs of

HF and AFs. Table S3. The oligonucleotides used in this study. Table S4. The primers used in this study.

Supplementary Material 2

Acknowledgements

Not applicable.

Author contributions

ZG: Formal analysis, Methodology, Investigation, Software, Validation, Writing-original draft, Writing-review & editing. QZ: Conceptualization, Data curation, Investigation, Writing-original draft. QL: Methodology, Analysis, Resources, Visualization. BS: Assistance, Investigation. YH: Analysis, Investigation. XS: Methodology, Assistance. QL: Supervision. XD: Conceptualization, Funding acquisition, Supervision, Project administration, Writing-original draft, Writing-review & editing. All authors read and approved the final manuscript.

Funding

This work was financially supported by the National Natural Science Foundation of China (32372839), the Fundamental Research Funds for the Central Universities (YDZX2024001), the Natural Science Foundation of Jiangsu Province (BK20231475), and Yaffe Technology Innovation and Service Program (2023kj08). None of these sponsors had any role in study design, collection, analysis, and interpretation of data.

Data availability

No datasets were generated or analysed during the current study.

Declarations

Ethics approval and consent to participate

All the animal-involved experiments in this study were conducted in accordance with the Chinese guidelines for administration of affairs concerning experimental animals and were reviewed, approved, and supervised by the Institutional Animal Ethics Committee of Nanjing Agricultural University (NJAU.No20220324059).

Consent for publication

Not applicable.

Competing interests

The authors declare no competing interests.

Received: 25 August 2024 / Accepted: 4 November 2024

Published online: 10 November 2024

References

1. Fiorentino G, Cimadomo D, Innocenti F, Soscia D, Vaiarelli A, Ubaldi FM, et al. Biomechanical forces and signals operating in the ovary during folliculogenesis and their dysregulation: implications for fertility. *Hum Reprod Update*. 2023;29(1):1–23.
2. Wu Y, Yang R, Lan J, Huang J, Fan Q, You Y, et al. Iron overload modulates follicular microenvironment via ROS/HIF-1 α /FSHR signaling. *Free Radic Biol Med*. 2023;196:37–52.
3. Gu L, Liu H, Gu X, Boots C, Moley KH, Wang Q. Metabolic control of oocyte development: linking maternal nutrition and reproductive outcomes. *Cell Mol Life Sci*. 2015;72(2):251–71.
4. Wang F, Liu Y, Ni F, Jin J, Wu Y, Huang Y, et al. BNC1 deficiency-triggered ferroptosis through the NF2-YAP pathway induces primary ovarian insufficiency. *Nat Commun*. 2022;13(1):5871.
5. Knapp E, Sun J. Steroid signaling in mature follicles is important for Drosophila ovulation. *Proc Natl Acad Sci U S A*. 2017;114(4):699–704.
6. Krause WC, Rodriguez R, Gegenhuber B, Matharu N, Rodriguez AN, Padilla-Roger AM, et al. Oestrogen engages brain MC4R signalling to drive physical activity in female mice. *Nature*. 2021;599:131–35.
7. Teoh JP, Li X, Simoncini T, Zhu D, Fu X. Estrogen-mediated gaseous signaling molecules in cardiovascular disease. *Trends Endocrinol Metab*. 2020;31(10):773–84.
8. Henriquez S, Kohen P, Xu X, Villarreal C, Munoz A, Godoy A, et al. Significance of pro-angiogenic estrogen metabolites in normal follicular development and follicular growth arrest in polycystic ovary syndrome. *Hum Reprod*. 2020;35(7):1655–65.
9. Dai X, Hong L, Shen H, Du Q, Ye Q, Chen X, et al. Estradiol-induced senescence of hypothalamic astrocytes contributes to aging-related reproductive function declines in female mice. *Aging*. 2020;12(7):6089–108.
10. van Hellemond IEG, Vriens JH, Peer PGM, Swinkels ACP, Smorenburg CH, Seynaeve CM, et al. Ovarian function recovery during anastrozole in breast cancer patients with chemotherapy-induced ovarian function failure. *J Natl Cancer Inst*. 2017;109(12):dx074.
11. Richards JS, Pangas SA. The ovary: basic biology and clinical implications. *J Clin Invest*. 2010;120(4):963–72.
12. Zhang J, Liu Y, Yao W, Li Q, Liu H, Pan Z. Initiation of follicular atresia: gene networks during early atresia in pig ovaries. *Reproduction*. 2018;156(1):23–33.
13. Sakaguchi K, Yanagawa Y, Yoshioka K, Suda T, Katagiri S, Nagano M. Relationships between the antral follicle count, steroidogenesis, and secretion of follicle-stimulating hormone and anti-müllerian hormone during follicular growth in cattle. *Reprod Biol Endocrinol*. 2019;17(1):88.
14. Talebi R, Ahmadi A, Afraz F, Sarry J, Plisson-Petit F, Genet C, et al. Transcriptome analysis of ovine granulosa cells reveals differences between small antral follicles collected during the follicular and luteal phases. *Theriogenology*. 2018;108:103–17.
15. Yang C, Song G, Lim W. Effects of endocrine disrupting chemicals in pigs. *Environ Pollut*. 2020;263:114505.
16. Zielonka L, Gajecka M, Lisieska-Zolnierczyk S, Dabrowski M, Gajecki MT. The effect of different doses of zearalenone in feed on the bioavailability of zearalenone and alpha-zearalenol, and the concentrations of estradiol and testosterone in the peripheral blood of pre-pubertal gilts. *Toxins*. 2020;12(3):144.
17. He Y, Wang T, Sun F, Wang L, Ji R. Effects of veterinary antibiotics on the fate and persistence of 17 β -estradiol in swine manure. *J Hazard Mater*. 2019;375:198–205.
18. Deng L, Min W, Guo S, Deng J, Wu X, Tong D, et al. Interference of pseudorabies virus infection on functions of porcine granulosa cells via apoptosis modulated by MAPK signaling pathways. *Virol J*. 2024;21(1):5.
19. Alfradique VAP, Netto DLS, Alves SVP, Machado AF, Novaes CM, Penitente-Filho JM, et al. The impact of FSH stimulation and age on the ovarian and uterine traits and histomorphometry of prepubertal gilts. *Domest Anim Endocrinol*. 2023;83:106786.
20. Shi S, Chu G, Zhang L, Yuan H, Madaniyati M, Zhou X, et al. Deubiquitinase UCHL1 regulates estradiol synthesis by stabilizing voltage-dependent anion channel 2. *J Biol Chem*. 2023;299:105316.
21. Rynkowska A, Stepniak J, Karbownik-Lewinska M. Fenton reaction-induced oxidative damage to membrane lipids and protective effects of 17 β -estradiol in porcine ovary and thyroid homogenates. *Int J Environ Res Public Health*. 2020;17:6841.
22. Liu J, Li X, Yao Y, Li Q, Pan Z. miR-1275 controls granulosa cell apoptosis and estradiol synthesis by impairing LRH-1/CYP19A1 axis. *Biochim Biophys Acta Gene Regul Mech*. 2018;1861(3):246–57.
23. Wang M, Wang Y, Yang L, Du X, Li Q. Nuclear lncRNA NORF reduces E2 release in granulosa cells by sponging the endogenous small activating RNA miR-339. *BMC Biol*. 2023;21(1):221.
24. Kopp F, Mendell JT. Functional classification and experimental dissection of long noncoding RNAs. *Cell*. 2018;172(3):393–407.
25. Geng X, Zhao J, Huang J, Li S, Chu W, Wang WS, et al. lnc-MAP3K13-7:1 inhibits ovarian GC proliferation in PCOS via DNMT1 downregulation-mediated CDKN1A promoter hypomethylation. *Mol Ther*. 2021;29(3):1279–93.
26. Liu SJ, Dang HX, Lim DA, Feng FY, Maher CA. Long noncoding RNAs in cancer metastasis. *Nat Rev Cancer*. 2021;21(7):446–60.
27. Zhou X, He Y, Pan X, Quan H, He B, Li Y, et al. DNMT1-mediated lncRNA IFFD controls the follicular development via targeting GLI1 by sponging miR-370. *Cell Death Differ*. 2023;30(2):576–88.
28. Zhou X, He Y, Quan H, Pan X, Zhou Y, Zhang Z, et al. HDAC1-mediated lncRNA stimulatory factor of follicular development to inhibit the apoptosis of granulosa cells and regulate sexual maturity through miR-202-3p-COX1 axis. *Cells*. 2023;12(23):2734.
29. Du X, Liu L, Li Q, Zhang L, Pan Z. NORFA, long intergenic noncoding RNA, maintains sow fertility by inhibiting granulosa cell death. *Commun Biol*. 2020;3(1):131.
30. Du X, Li Q, Yang L, Zeng Q, Wang S. Transcriptomic data analyses reveal that sow fertility-related lincRNA NORFA is essential for the normal states and functions of granulosa cells. *Front Cell Dev Biol*. 2021;9:610553.
31. Jia Y, Domenico J, Takeda K, Han J, Wang M, Armstrong M, et al. Steroidogenic enzyme Cyp11a1 regulates type 2 CD8+ T cell skewing in allergic lung disease. *Proc Natl Acad Sci U S A*. 2013;110(2):8152–57.
32. Du X, Pan Z, Li Q, Liu H, Li Q. SMAD4 feedback regulates the canonical TGF- β signaling pathway to control granulosa cell apoptosis. *Cell Death Dis*. 2018;9(2):151.
33. Li Q, Huo Y, Wang S, Yang L, Li Q, Du X. TGF- β 1 regulates the lncRNA transcriptome of ovarian granulosa cells in a transcription activity-dependent manner. *Cell Prolif*. 2023;56:e13336.
34. Du X, Liu L, Wu W, Li P, Pan Z, Zhang L, et al. SMARCA2 is regulated by NORFA/miR-29c, a novel pathway related to female fertility, controls granulosa cell apoptosis. *J Cell Sci*. 2020;133(23):jcs249961.
35. Foissac S, Djebali S, Munyard K, Vialaneix N, Rau A, Muret K, et al. Multi-species annotation of transcriptome and chromatin structure in domesticated animals. *BMC Biol*. 2019;17(1):108.
36. Liu Z, Han S, Shen X, Wang Y, Cui C, He H, et al. The landscape of DNA methylation associated with the transcriptomic network in layers and broilers generates insight into embryonic muscle development in chicken. *Int J Biol Sci*. 2019;15(7):1404–18.
37. Jia H, Wu Z, Tan J, Wu S, Yang C, Raza SHA, et al. lnc-TRTMFS promotes milk fat synthesis via the miR-132x/RAI14/mTOR pathway in BMECs. *J Anim Sci*. 2023;101:skad218.
38. Zhang Y, Li F, Shi Y, Zhang T, Wang X. Comprehensive transcriptome analysis of hair follicle morphogenesis reveals that lncRNA-H19 promotes dermal papilla cell proliferation through the chi-miR-214-3p/ β -catenin axis in Cashmere Goats. *Int J Mol Sci*. 2022;23(7):10006.
39. Lv W, Jiang W, Luo H, Tong Q, Niu X, Liu X, et al. Long noncoding RNA lncMREF promotes myogenic differentiation and muscle regeneration by interacting with the Smarca5/p300 complex. *Nucleic Acids Res*. 2022;50(18):10733–55.
40. Li M, Chai HF, Peng F, Meng YT, Zhang LZ, Zhang L, et al. Estrogen receptor beta upregulated by lncRNA-H19 to promote cancer stem-like properties in papillary thyroid carcinoma. *Cell Death Dis*. 2018;9(11):1120.
41. Li Y, Zhang J, Liu YD, Zhou XY, Chen X, Zhe J, et al. Long non-coding RNA TUG1 and its molecular mechanisms in polycystic ovary syndrome. *RNA Biol*. 2020;17(12):1798–810.
42. Knapczyk-Stwora K, Nynca A, Ciereszko RE, Pauksztó L, Jastrzebski JP, Czaja E, et al. Transcriptomic profiles of the ovaries from piglets neonatally exposed to 4-tert-octylphenol. *Theriogenology*. 2020;153:102–11.
43. Lin YC, Papadopoulos V. Neurosteroidogenic enzymes: CYP11A1 in the central nervous system. *Front Neuroendocrinol*. 2021;62:100925.
44. Okada M, Lee L, Maekawa R, Sato S, Kajimura T, Shinagawa M, et al. Epigenetic changes of the Cyp11a1 promoter region in granulosa cells undergoing luteinization during ovulation in female rats. *Endocrinology*. 2016;157(9):3344–54.
45. Shi D, Zhou X, Cai L, Wei X, Zhang L, Sun Q, et al. Placental DNA methylation analysis of selective fetal growth restriction in monochorionic twins reveals aberrant methylated CYP11A1 gene for fetal growth restriction. *FASEB J*. 2023;37(10):e23207.

46. Lavoie HA, King SR. Transcriptional regulation of steroidogenic genes: STARD1, CYP11A1 and HSD3B. *Exp Biol Med.* 2009;234(8):880–907.
47. Wang M, Wang Y, Yao W, Du X, Li Q. Lnc2300 is a cis-acting long non-coding RNA of CYP11A1 in ovarian granulosa cells. *J Cell Physiol.* 2022;237(11):4238–50.
48. An X, Ma H, Liu Y, Li F, Song Y, Li G, et al. Effects of Mir-101-3p on goat granulosa cells in vitro and ovarian development in vivo via STC1. *J Anim Sci Biotechnol.* 2020;11:102.
49. Huo Y, Li Q, Yang L, Li X, Sun C, Liu Y, et al. SDNOR, a novel antioxidative lncRNA, is essential for maintaining the normal state and function of porcine follicular granulosa cells. *Antioxidants.* 2023;12(4):799.
50. Guo H, Golczer G, Wittner BS, Langenbucher A, Zachariah M, Dubash TD, et al. NR4A1 regulates expression of immediate early genes, suppressing replication stress in cancer. *Mol Cell.* 2021;81(19):4041–58.
51. Guzman A, Hughes CHK, Murphy BD. Orphan nuclear receptors in angiogenesis and follicular development. *Reproduction.* 2021;162(3):R35–54.
52. Liu Y, Zhang P, Wu Q, Fang H, Wang Y, Xiao Y, et al. Long non-coding RNA NR2F1-AS1 induces breast cancer lung metastatic dormancy by regulating NR2F1 and DeltaNp63. *Nat Commun.* 2021;12(1):5232.
53. Guan YF, Huang QL, Ai YL, Chen QT, Zhao WX, Wang XM, et al. Nur77-activated lncRNA WFDC21P attenuates hepatocarcinogenesis via modulating glycolysis. *Oncogene.* 2020;39(11):2408–23.
54. Meinsohn MC, Smith OE, Bertolin K, Murphy BD. The Orphan nuclear receptors steroidogenic factor-1 and liver receptor homolog-1: structure, regulation, and essential roles in mammalian reproduction. *Physiol Rev.* 2019;99(2):1249–79.
55. Hu K, Wang C, Xu Y, Li F, Han X, Song C, et al. Interaction of lncRNA Gm2044 and EEF2 promotes estradiol synthesis in ovarian follicular granulosa cells. *J Ovarian Res.* 2023;16(1):171.
56. Hu K, He C, Ren H, Wang H, Liu K, Li L, et al. lncRNA Gm2044 promotes 17 β -estradiol synthesis in mGCs by acting as mir-138-5p sponge. *Mol Reprod Dev.* 2019;86(3):1023–32.
57. Vierbuchen T, Agarwal S, Johnson JL, Galia L, Lei X, Stein K, et al. The lncRNA LUCAT1 is elevated in inflammatory disease and restrains inflammation by regulating the splicing and stability of NR4A2. *Proc Natl Acad Sci U S A.* 2023;120(1):e2213715120.
58. Wang P, Xue Y, Han Y, Lin L, Wu C, Xu S, et al. The STAT3-binding long non-coding RNA lnc-DC controls human dendritic cell differentiation. *Science.* 2014;344(6181):310–3.
59. Jiang T, Qi J, Xue Z, Liu B, Liu J, Hu Q, et al. The m6A modification mediated-lncRNA POU6F2-AS1 reprograms fatty acid metabolism and facilitates the growth of colorectal cancer via upregulation of FASN. *Mol Cancer.* 2024;23(1):55.

Publisher's note

Springer Nature remains neutral with regard to jurisdictional claims in published maps and institutional affiliations.